A NOVEL APPROACH TO ANALYSIS OF NONLINEAR CIRCUITS EXCITED BY MODULATED SIGNALS

Amir Vaezi, Abdolali Abdipour, Abbas Mohammadi

Microwave/mm-Wave & Wireless Communication Research Lab,
Radio Communication Centre of Excellence, dElectrical Engineering Department,
Amirkabir University of Technology, Tehran, Iran

Key words: ET-HB, nonlinear circuits, modulated signals

Abstract: In this paper, a new formulation to Envelope Transient Harmonic Balance (ET-HB) method is proposed that is appropriate to analysis nonlinear active microwave circuits. This formulation uses an ET-HB with small value of time step during the transient time and a classic HB method after the transient. This highly reduces the time consuming classic ET-HB computation time. As an example, we applied this method to analyze a power amplifier where it is driven by QPSK and 16-QAM modulated signals. The spectral growth, error vector magnitude symbol error rate degradation, and constellation performance reduction due to nonlinearity of the power amplifier are studied using the proposed technique. The obtained results show that the proposed technique can be efficiently used to analyze and simulation of the nonlinear microwave circuits when they are used in modern wireless standards.

Nov pristop k analizi nelinearnih vezij vzbujanih z moduliranimi signali

Kjučne besede: ET-HB, nelinearna vezja, modulirani signali

Izvleček: V članku je predstavljen nov pristop k metodi ET-HB, ki je primerna za analizo nelinearnih aktivnih mikrovalovnih vezij. Ta metoda uporablja majhne vrednosti časovnega koraka med prehodnim pojavom, kar močno zmanjša čas potreben za izračune. Kot primer smo to metodo uporabili za analizo močnostnega ojačevalnika vzbujanega z QPSK in 16-QAM modulirnimi signali. Dobljeni rezultati pričajo, da predlagano metodo lahko uspešno uporabimo za analizo in simulacijo nelinearnih mikrovalovnih vezij.

1. Introduction

To achieve high bandwidth (BW) efficiency, new standards such as WiMAX and WCDMA use complex modulation schemes such as a quadrature phase-shift keying (QPSK) and quadrature amplitude modulation QAM /1,2/. Nowadays, engineers seek for simulation methods and test procedures closer to the system's final operation regime. Actually, telecommunications signals are usually composed of the carrier modulated by information signals (i.e., signals that are necessarily aperiodic in time), and presenting band-limited continuous spectra /3/. Due to analyze circuits exited by these digital modulated signals, accurate and reliable CAD tools and numerical algorithms are one of the main challenging aspects of modern communication systems. A number of methods exist for numerical analysis of such systems. As discussed in /4/, Since the excitation is a multi-rate signal with widely separated rates, the time domain - the most effective method for transient response - has difficulty. Because, simulating the slowest signal component period, time-steps need to be smaller than the period of the fastest so leads to a large number of time point and increases simulation time, enormously. On the other hand, Harmonic Balance (HB), an efficient method to analyze the microwave circuits, is only applicable to periodic (or quasi-periodic) systems. Therefore, mixed mode techniques are seemed to be efficient. In fact, in these methods like Envelope Transient HB (ET-HB) or Circuit Envelope, the high frequency dynamic is treated by microwave steady state simulator like HB and the low frequency dynamic with time domain (TDI). In the literature several formulations were presented /5-16/.

In this paper, a novel closed formulation of Envelope Transient HB appropriate for analysis of nonlinear active microwave circuits and systems is proposed. This formulation form enables using adaptive time scales, resulting in saving in simulation time. Then, as an example of application, a linear power amplifier in WiMAX technology frequency band is presented, and then the simulation results using this method are compared with other methods. Finally, using the proposed CAD, we considered the effect of the nonlinearity of the power amplifier when driven with 16-QAM and QPSK modulated signals on the system performance.

2. Theoretical formulation

Modulated signal in which the information signal is typically aperiodic and has a spectral content of much lower frequency than the periodic carrier, is a practical example of multi-rate signals /4/. When the circuit is faced to this type of signals, it will be possible to use mixed mode simulation techniques, handling the solution dependence of some of its time and variables in time-domain, and the course of the solution to other time variable in frequency domain.

If we consider a modulated carrier driving signal, exciting signal $v_s(t)$ in the circuit may be written as equation (1):

$$v_s(t) = v_m(t)(e^{-j2\pi f_c t} + e^{j2\pi f_c t}) \quad (1)$$

Where f_c is carrier frequency and $v_m(t)$ represents the envelope (modulating) signal. Considering a multi-time representation for $v_s(t)$, constructed as follows, for the slow varying parts of the expression for $v_s(t)$, t is replaced by t_s, and for the fast varying parts, t_c. the resulting function of two variables is denoted by $v_s(t_s, t_c)$.

$$\hat{v}_s(t_s, t_c) = v_m(t_s)(e^{-j2\pi f_c t_c} + e^{j2\pi f_c t_c}) \quad (2)$$

Given an active nonlinear circuit under modulated excitation including linear and nonlinear elements, it can be subdivided into two, nonlinear and linear part /4,5/. The multi rate representation of differential equation of the circuit leads to a new version of HB equation, a multi partial differential equation as follows:

$$\boldsymbol{f}_{NL}(\boldsymbol{v}(t_s,t_c)) = \boldsymbol{i}_L(t_s,t_c) + \frac{\partial \boldsymbol{q}_{nl}(\boldsymbol{v}(t_s,t_c))}{\partial t_c} + \frac{\partial \boldsymbol{q}_{nl}(\boldsymbol{v}(t_s,t_c))}{\partial t_s} + \boldsymbol{i}_{nl}(\boldsymbol{v}(t_s,t_c)) + \boldsymbol{i}_S(t_s,t_c) = \boldsymbol{0} \quad (3)$$

Where, $\boldsymbol{v}$ *is* the vector of port voltages; $\boldsymbol{i}_S$ the vector of source contributions at ports; $\boldsymbol{i}_L(t_s, t_c)$ the vector of linear part current and $\boldsymbol{i}_{nl}$, $\boldsymbol{q}_{nl}$ define the contributions of nonlinear reactive and conductive elements, respectively.

Since eq.(3) is periodic respect to the t_c, applying Fourier series, it is reduced to:

$$\mathbf{F}_{NL}(\mathbf{V}(t_s)) = \mathbf{I}_L(t_s) + j\boldsymbol{\Omega}\mathbf{Q}_{nl}(\mathbf{V}(t_s)) + \frac{\partial \mathbf{Q}_{nl}(\mathbf{V}(t_s))}{\partial t_s} + \mathbf{I}_{nl}(\mathbf{V}(t_s)) + \mathbf{I}_S(t_s) = \mathbf{0} \quad (4)$$

Where, its components are vectors of time-varying Fourier series coefficients, $V(t_s)$ is the vector of unknowns where

$$v(t_s, t_c) = \sum_{k=-K}^{k=K} V_k(t_s) \cdot e^{jk\omega_0 t_c}$$

$$V_k(t_s) = \frac{1}{2\pi} \int_{-\frac{BW}{2}}^{\frac{BW}{2}} V_k(\omega_s) \cdot e^{j\omega_s t} d\omega_s$$

So, $V_k(t_S)$ is time variant complex envelope of the *k'th* harmonic of carrier frequency ω_c, BW is the largest bandwidth of the carrier frequency envelopes. So, in the standard form of piecewise HB circuit with N nonlinear elements (figure 2) the time varying vectors in Eq (4) presented as: $V(t_s) = [V_1(t_s) \; K \; V_n(t_s) \; V_N(t_s)]^T$ and $V_n(t_s) = [V_{n0}(t_s) \; K \; V_{nK}(t_s) \ldots V_{nK}(t_s)]^T$. And Ω is a diagonal matrix of harmonics of carrier frequency. As follows:

$$\boldsymbol{\Omega} = \begin{bmatrix} \boldsymbol{\omega}_n & \boldsymbol{O} & \Lambda & \boldsymbol{O} \\ \boldsymbol{O} & \boldsymbol{\omega}_n & \boldsymbol{O} & \boldsymbol{M} \\ \boldsymbol{M} & \boldsymbol{O} & \boldsymbol{O} & \boldsymbol{O} \\ \boldsymbol{O} & \Lambda & \boldsymbol{O} & \boldsymbol{\omega}_n \end{bmatrix}, \quad \boldsymbol{\omega}_n = \begin{bmatrix} 0 & 0 & \Lambda & 0 \\ 0 & \omega_c & 0 & \mathrm{M} \\ \mathrm{M} & 0 & 0 & 0 \\ 0 & \Lambda & 0 & K\omega_c \end{bmatrix}$$

and $\boldsymbol{O} = \boldsymbol{O}_{(K+1)\times(K+1)}$ is a zero matrix.

In piecewise harmonic balance I_L should be evaluated. Since linear part matrix, Y_L is only realized in frequency domain, so $I_L(\omega_s, \omega_c) = Y_L(\omega_s, \omega_c)V(\omega_s, \omega_c)$. In which ω_S is related to t_s . $t_s \Leftrightarrow \omega_s$.

It can be proven that by restricting the envelope dynamics to be slow compared with the carrier, $I_L(t_s, \omega_c)$ is calculated as follows (it is truncated to the order of R_T): /5/

$$I_{Lk}(t_s) = \sum_{R=0}^{R_T} \left[\frac{1}{n! j^R} \frac{d^R Y_L(\omega)}{d\omega^R}\bigg|_{\omega=k\omega_c} \frac{\partial^R V_k(t_s)}{\partial t_s^R} \right] \quad (5)$$

An appropriate discretization for t_S, leads to the complete set of (2K+1) differential equation, converted into a conventional HB equation for each time sample. Using backward difference (Euler rule),

$$\frac{\partial \boldsymbol{Q}_{nl}(\boldsymbol{V}(t_s))}{\partial t_s}\bigg|_{t_s=t_{si}} = \frac{\boldsymbol{Q}_{nl}(\boldsymbol{V}(t_{si})) - \boldsymbol{Q}_{nl}(\boldsymbol{V}(t_{s\,i-1}))}{\Delta t_s} \quad (6)$$

$$\frac{\partial^R \boldsymbol{V}_k(t_s)}{\partial t_s^R}\bigg|_{t_s=t_{si}} = \frac{1}{(\Delta t_s)^R} \sum_{r=0}^{R} \left[(-1)^r \binom{R}{R-r} \boldsymbol{V}(t_{s\,i-r}) \right] \quad (7)$$

And also applying this rule to eq (4). We have:

$$\boldsymbol{F}_{NL}(\boldsymbol{V}(t_{si})) = \sum_{R=0}^{R_T} \left\{ \frac{1}{n! j^R} \frac{d^R \boldsymbol{Y}_L(\omega)}{d\boldsymbol{\omega}^R}\bigg|_{\omega=\omega_k} \frac{1}{(\Delta t_s)^R} \sum_{r=0}^{R} \left[(-1)^r \binom{R}{R-r} \boldsymbol{V}(t_{s\,i-r}) \right] \right\} + j\boldsymbol{\Omega}\boldsymbol{Q}_{nl}(\boldsymbol{V}(t_{si})) + \frac{\boldsymbol{Q}_{nl}(\boldsymbol{V}(t_{si})) - \boldsymbol{Q}_{nl}(\boldsymbol{V}(t_{s\,i-1}))}{\Delta t_s} + \boldsymbol{I}_{nl}(\boldsymbol{V}(t_{si})) + \boldsymbol{I}_S(t_{si}) = \boldsymbol{0} \quad (8)$$

Where $\boldsymbol{\omega}_k = [0 \; \Lambda \; K\omega_c]^T$.

$$\boldsymbol{F}_{NL}(\boldsymbol{V}(t_{si})) = \boldsymbol{Y}_L^{ET} \boldsymbol{V}(t_{si}) + j\boldsymbol{\Omega}^{ET}\boldsymbol{Q}_{nl}(\boldsymbol{V}(t_{si})) + \boldsymbol{I}_{nl}(\boldsymbol{V}(t_{si})) + \boldsymbol{I}_S(t_{si}) + \boldsymbol{I}_{i-1} = \boldsymbol{0} \quad (9-a)$$

$$\boldsymbol{Y}_L^{ET} = \sum_{R=0}^{R_T} \left\{ \frac{1}{n! j^R} \frac{d^R \boldsymbol{Y}_L(\omega)}{d\boldsymbol{\omega}^R}\bigg|_{\omega=\omega_k} \frac{1}{(\Delta t_s)^R} \right\}$$

$$\boldsymbol{\Omega}^{ET} = \boldsymbol{\Omega} + \frac{\boldsymbol{1}}{\Delta t_s}$$

$$\boldsymbol{I}_{i-1} = \sum_{R=0}^{R_T} \left\{ \frac{1}{n! j^R} \frac{d^R \boldsymbol{Y}_L(\omega)}{d\boldsymbol{\omega}^R}\bigg|_{\omega=\omega_k} \frac{1}{(\Delta t_s)^R} \left(\sum_{r=1}^{R} \left[(-1)^r \binom{R}{R-r} \boldsymbol{V}(t_{s\,i-r}) \right] \right) \right\} + \frac{-\boldsymbol{Q}_{nl}(\boldsymbol{V}(t_{s\,i-1}))}{\Delta t_s} \quad (9)$$

Where, $\boldsymbol{1}$ is a unit matrix. As we can see in eq (9-a), this equation is similar to $\boldsymbol{F(V)}$, ordinary HB equation. There are some differences in $\boldsymbol{Y}_L^{ET}$, $\boldsymbol{I}_{i-1}$ and $\boldsymbol{\Omega}^{ET}$ described. As we can see in Eq.(9), $\boldsymbol{I}_{i-1}$ must be calculated from previous time steps. So, solving this equation for each time step,

leads to the varying envelope of desirable voltage at harmonics of carrier frequency.

Assuming Eq (5) with order of R_T, Enables analysis of nonlinear circuits excited by arbitrary bandwidth. So the simulation leads to more accurate results.

2.1. Small Band Modulating Signals

The case of most practical interest to microwave and wireless systems is the one in which the modulating signals are very slowly varying signals, $BW << f_c$, the calculation converges for $R_T \geq 1$. Thus, by assuming $R_T=1$, calculation for each time step only requires knowing at one previous time step results. So Y_L^{ET} and I_{i-1} in Eq.(9) can be reduced to:

$$Y_L^{ET} = Y_L + \frac{1}{j\Delta t_s}\frac{dY(\omega)}{d\omega}\bigg|_{\omega=\omega_k}$$

$$I_{i-1} = \frac{1}{j}\frac{dY(\omega)}{d\omega}\bigg|_{\omega=\omega_k}\frac{-V(t_{s\,i-1})}{\Delta t_s} + \frac{-Q_{nl}(V(t_{s\,i-1}))}{\Delta t_s} \quad (10)$$

2.2. Adaptive Time Scales

Let consider eq (8) for example with $R_T=1$, where $Q_{nl}(V(t_{si})) = Q_{nl}(V(t_{s\,i-1}))$, with this assumption, the Eq (8) converts to a common Harmonic Balance equation. In this case we don't need to solve the equation for *i+1* step if $I_S(t_{si}) = I_S(t_{s\,i+1})$ (results in $V(t_{si}) = V(t_{s\,i-1})$). This means that we can assume Δt_s small enough to fallow the input transient effects precisely and after ending transient effects, we can use a HB instead of many ET-HB routines. Therefore using this technique, if we choose adaptive time steps, Δt_s^j, also, it will offer some improvement in efficiency and time-saving, to follow the input transient effects and also evaluate the steady state response of microwave circuits containing waveforms with sharp edge and spikes in which; For spikes and sharp edges of waveform we choose Δt_s very small and for smooth parts of signal larger amounts of Δt_s is chosen. Using this method, results in a good saving in simulation time (it will be explained in the next part). The improvement in efficiency may be observed in some circuits more clear than others e.g. PLLs transient responses can be efficiently observed using this technique.

3. Simulation and Results

In this section as an example of application, a one-stage class A power amplifier with 17 dB of gain and output power of 18 dBm suitable for use in Fixed WiMAX technology based on IEEE 802.16 d standard is studied. It is designed to work with 200MHz bandwidth centered at frequency of 3.5 GHz. The amplifier includes input and output Microstrip matching networks and the necessary DC bias circuitry. The Pseudomorahic InGaAs/ AlGaAS/GaAs HEMT /17/ is used to realized power amplifier. According to reduction of harmonic distortion on output power, it is biased in class A so V_d =6 V and V_g =0 V is chosen (Standard schematic of the power amplifiers). Matching networks are designed and optimized to obtain maximum output power and minimum possible harmonic distortion. So, simulating circuit under one-sinusoidal tone excitation using HB, results in 1-dB compression point of P_{1dB}= 18.7 with an associated Gain of 17 dB and PAE of nearly 20%. This is illustrated in figure 2.

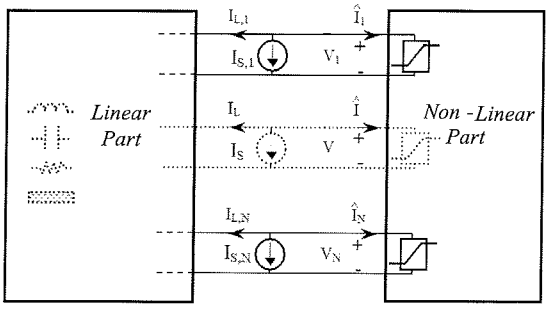

Fig. 2. Deviding a nonlinear circuit by a linear and nonlinear part.

As the second step, the designed power amplifier should be exited by a modulated signal. due to confirm the formulation and CAD presented, first, it is applied to the circuit derived with a RF pulse source (modulated source), creates a pulse modulated RF carrier with frequency of f_c (with rise-time, fall-time and width of constant portion of pulse of 0.25, 0.25 and 3 n sec, respectively). Accordingly, the absolute value of output voltage evaluated with proposed CAD is confirmed with Time-Domain simulation. It is shown in figure 3. ET-HB in comparison to time domain techniques proposes a more fast simulation. In addition, using adaptive time steps, Δt_s^j, for spikes and sharp edges of waveform we chose Δt_s very small and for smooth parts of signal, larger amounts of Δt_s is chosen. Consequently, in this case, led to more time saving about 68 percent.

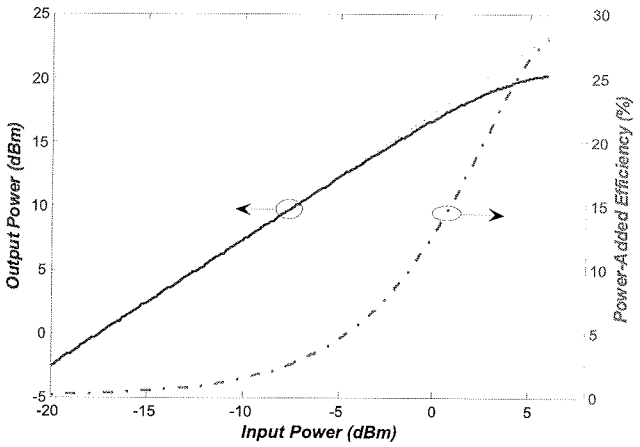

Fig. 3. Output power and Power added Efficiency of the amplifier versus input signal level.

Now, we can consider analysis of designed amplifier with modulated excitation using proposed CAD formulation. Since, One of the important digital modulation schemes, allowed in IEEE 802.16 standard (*WirelessMAN-SCa*), is

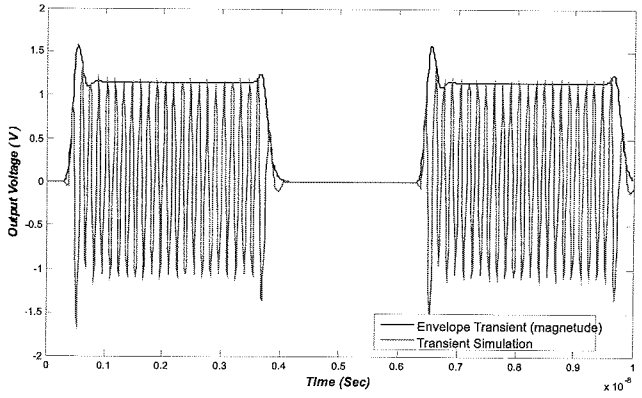

Fig. 4. Proposed CAD results comply with Time domain simulation.

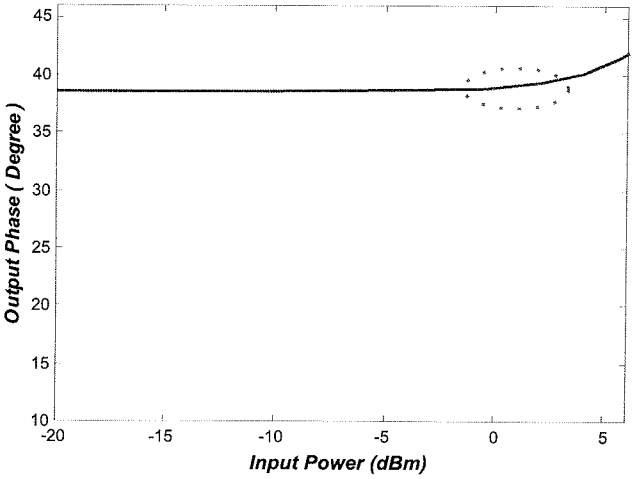

Fig. 5. Plot of simulation excess phase-shift versus input drive level, for illustrating AM-PM characterization.

16-QAM, so, we have considered an input excitation of a modulated signal at 3.5 GHz. Modulating signal, a 16-QAM symbol stream, is responsible for the envelope of the RF carrier. Applying proposed CAD, we can consider the adverse effect of nonlinearity of the power amplifier on modulated signal and then, on output demodulated signal. The input signal was first set at a power that was low-enough to prevent strong nonlinearity (maximum of input power was much set lower than $P_{1\ dB}$). Regarding the constellation diagram of the output voltage signal, we can understand that a phase shift of about 40 degrees with comparison of constellation diagram of input is apparent. This phase variation may be related to the AM-PM conversion. As it is depicted in figure 5, the calculating AM-PM conversion confirms this subject. The constellation diagram of the input and output envelope at P_{1dB} is shown in figure 6-a. Figure 6-c presents the input and output time domain envelope signal. Spectrum of the output signal for 16-QAM is shown in figure 6-d. Note that the phase shift is compensated and amounts are normalized (with small signal gain) in all presented constellation diagrams.

(a)

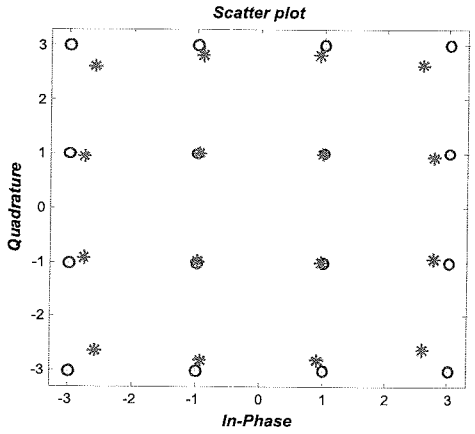

(b)

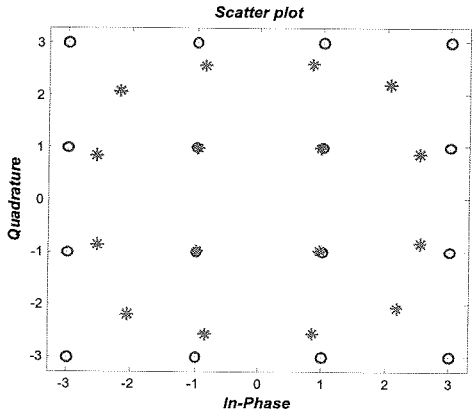

(c)

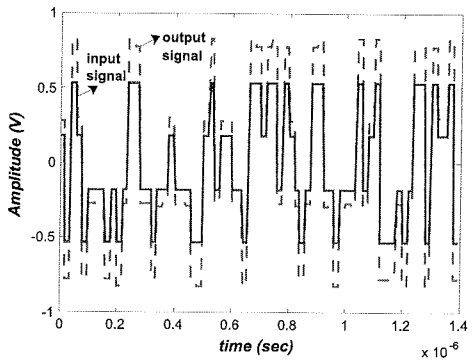

(d)

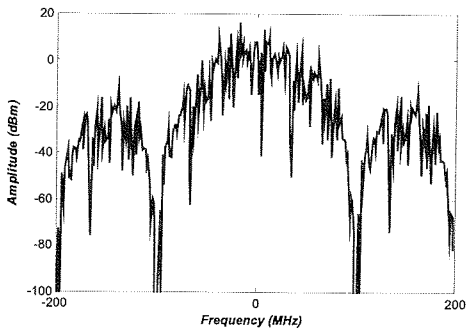

Fig. 6. (a) Constellation diagram @ P_{1dB} (circles: input diagram; stars: output diagram), (b) Constellation diagram @ P_{1dB} +3 (circles: input diagram; stars: output diagram), (c) time-domain envelope (solid line: input signal; dotted line: output signal scaled with 2.5) and (d) spectrum of the output signal for 16-QAM.

Increasing the input power up to P_{1dB} or more causes more distortion especially in gain. So, the constellation changes. Figure 6-b shows constellation of output voltage with input power of (P_{1dB}+3) dBm. By focusing more on this figure, as we expected, we realized that the symbols with larger magnitude due to lower gain have larger variance in respect to its relative position. Therefore, increasing the input power changes the arrangement of symbols in constellation diagram.

The Error Vector Magnitude (EVM) defines the average constellation error with respect to the farmost constellation point power, and defined by following equation /18/:

$$EVM = \sqrt{\frac{\frac{1}{N}\sum_{1}^{N}(\Delta I^2 - \Delta Q^2)}{S_{\max}^2}} \qquad (11)$$

Where, N is the number of symbols in the measurement period and S_{max} the maximum constellation amplitude.

EVM diagram for 16-QAM modulation schemes versus various input power is shown in figure 7. Enlarging the input power leads to stronger nonlinearity and consequently, the EVM increases.

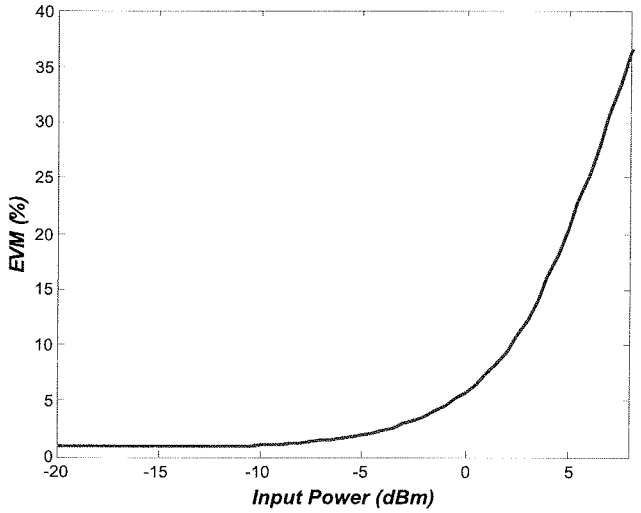

Fig. 7. Error Vector Magnitude versus input power

Also, this nonlinearity phenomenon causes a more symbol error rate (SER) in communication system. In the figure 8 we have shown the effect of nonlinearity of this power amplifier on SER of a 16-QAM signal through a noisy Gaussian channel. As it is illustrated, enlarging the input power results in worse Symbol Error Rates. Let consider QPSK, another modulation mode supported in IEEE 802.16 standard (WirelessMAN-SCa), for input excitation signal. PSK is a digital modulation where the carrier phase is keyed by the digital modulation signal. So, a finite number of phases are used. Therefore in the case of PSK, amplitude distortion (AM-AM) could not chiefly cause any defect. The main distortion could affect on system performance. Thus, have a flat AM-PM conversion characteristic,

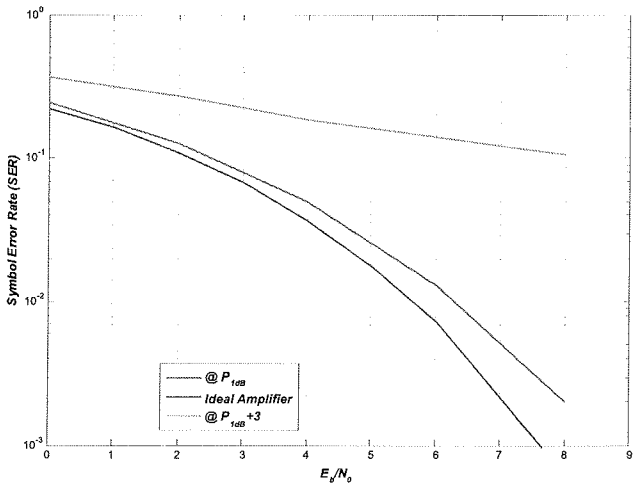

Fig. 8. SER through the Gaussian channel for 3 excitation power for 16-QAM

results in lower errors at the output of demodulator. The constellation diagram of the input and output envelope with QPSK modulation at P_{1dB} is shown in figure 9-a. Figure 9-b presents the input and output time domain envelope signal. Spectrum of the output signal for QPSK is shown in figure 9-c.

4. Conclusion

A new formulation of Envelope Transient HB appropriate for transient and steady state analysis of nonlinear active microwave circuits was presented. This novel approach enables using adaptive time scales resulting in fast simulation of microwave circuits. The performance of this method was investigated by applying on a microwave circuit. As an application of this method, a power amplifier in WiMAX frequency band excited by 16-QAM and QPSK modulated signal was considered. And the effect of nonlinearity on the output and system performance was discussed. As a result, we showed that QPSK is more resistant to the amplifier nonlinearity than QAM. It was shown that, enlarging the input power for 16-QAM results in worse Symbol Error Rate and Error vector magnitude.

5. Acknowledgement

This work is supported in part by Iran Telecommunication Research Center (ITRC)

References

/1/ A. B. Carlson, "*Communication Systems*", 4th Ed, McGraw-Hill, 2002.

/2/ J. G. Proakis, M. Salehi, "*Digital Communications*", 5. th. Edition, McGraw-Hill, 2008

/3/ Kenington, P., *"High-Linearity RF Amplifier Design"*, Norwood, MA: Artech House, 2000.

/4/ J. Roychowdhury, *"Effcient Methods for Simulating Highly Nonlinear Multi-Rate Circuits"* IEEE Trans. Circuits Syst. I, Fundam. Theory Appl., 2001.

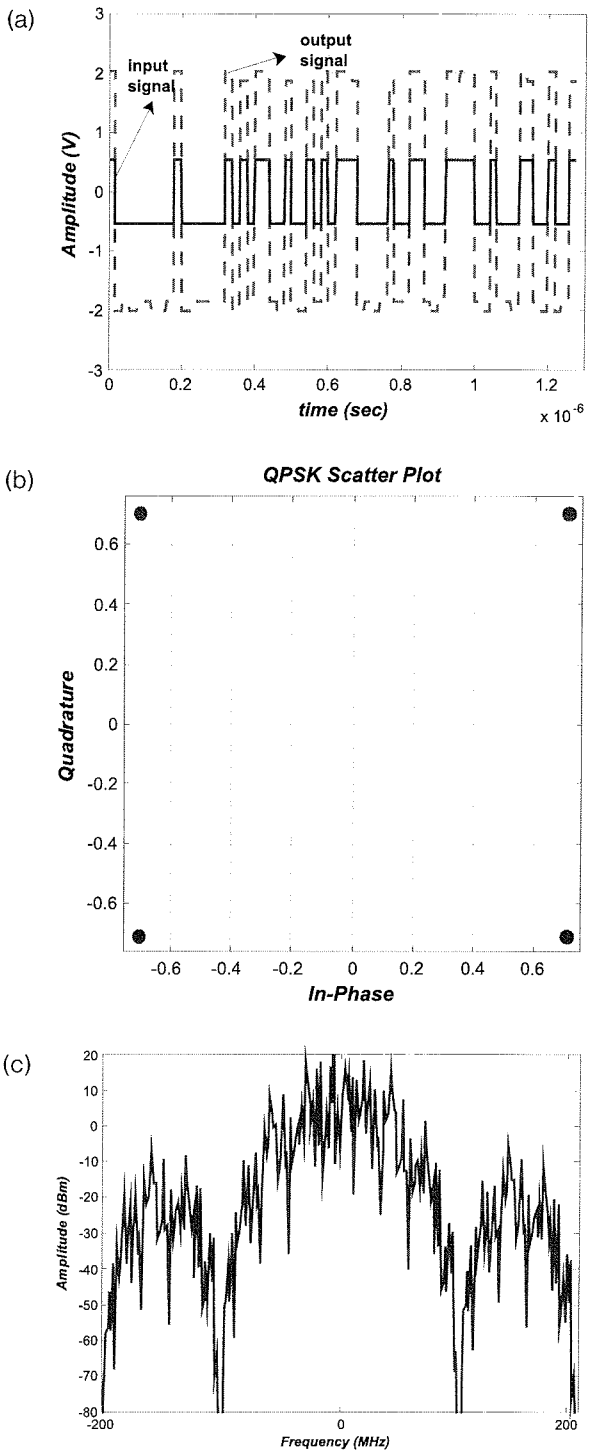

Fig. 9. (a) Constellation diagram @ P_{1dB} (circles: input diagram; stars: output diagram), (b) time-domain envelope (solid line: input signal; dotted line: output signal) and (c) output and input signals and spectrum of the output signal for QPSK.

/5/ J.C. Pedro and N.B. Carvalho, ***"Intermodulation distortion in microwave and wireless circuits"***, Artech House, Norwood, MA 2003.

/6/ Kundert, K.S.; Sorkin, G.B.; Sangiovanni-Vincentelli,A, ***"Applying harmonic balance to almost-periodic circuits"*** Microwave Theory and Techniques, IEEE Transactions on Volume 36, Issue 2, Feb 1988 Page(s):366 - 378

/7/ E. Ngoya and R. Larchevčque, ***"Envelope transient analysis: a new method for the transient and steady-state analysis of microwave communications circuits and systems,"*** in IEEE MTT-S Int. Microw. Symp. Dig., San Francisco, CA, Jun. 1996, pp. 1365-1368.

/8/ S. Sancho, A. Suarez, and J. Chuan, ***"General envelope-transient formulation of phase-locked loops using three time scales,"*** IEEE Trans. Microw. Theory Tech., vol. 52, no. 4, pp. 1310-1320, Apr. 2004.

/9/ H. Vahdati, A. **Abdipour**, ***"Nonlinear stability analysis of microwave oscillators using circuit envelope technique"***, will be appeared in journal of Transaction, on IEICE, vol E92-e, No.2 Feb**2009**,

/10/ Carvalho, N.B.; Pedro, J.C.; Jang, W.; Steer, M.B. ***,"Nonlinear RF circuits and systems simulation when driven by several modulated signals"*** Microwave Theory and Techniques, IEEE Transactions on Volume 54, Issue 2, Feb. 2006 Page(s): 572 - 579

/11/ V. Rizzoli, A. Neri, and F. Mastri, *"A modulation-oriented piecewise harmonic-balance technique suitable for transient analysis and digitally modulated signals,"* in Proc. 26th Eur. Microw. Conf., Prague, Czech Republic, Sep. 1996, pp. 546-550.

/12/ J. C. Pedro and N. B. Carvalho, *"Simulation of RF circuits driven by modulated signals without bandwidth constraints,"* in IEEE MTT-S Int.Microw. Symp. Dig., Seattle, WA, Jun. 2002, pp. 2173-2176.

/13/ M. Condon and E. Dautbegovic, *"Anovel envelope simulation technique for high-frequency nonlinear circutis,"* in Proc. 33rd Eur. Microw. Conf., Munich, Germany, Oct. 2003, pp. 619-622.

/14/ D. Sharrit, "Method for Simulating a Circuit," U.S. Patent 5 588 142, May 12, 1995.

/15/ N. B. Carvalho, J. C. Pedro, W. Jang, and M. B. Steer, "Nonlinear simulation of mixers for assessing system-level performance," Int. J. RF Microw. Computer-Aided Eng.

/16/ V. Rizzoli, A. Neri, F. Mastri, and A. Lipparini, "Modulation-oriented harmonic balance based on Krylov-subspace methods," in IEEE MTT-S Int. Microw. Symp. Dig., Jun. 1999, pp. 771-774.

/17/ Siddiqui, M.K.; Sharma, A.K.; Callejo, L.G.; Lai, R.,***"A high-power and high-efficiency monolithic power amplifier at 28GHz for LMDS applications"*** Microwave Theory and Techniques, IEEE Transactions on Volume 46, Issue 12, Dec 1998 Page(s):2226 - 2232

/18/ IEEE Std 802.16™-2004 (Revision of IEEE Std 802.16-2001, IEEE Standard for Local and metropolitan area networks, Part 16: Air Interface for Fixed Broadband Wireless Access Systems, Approved 24 June 2004.

Amir Vaezi, Abdolali Abdipour, Abbas Mohammadi

Microwave/mm-Wave & Wireless Communication Research Lab, Radio Communication Centre of Excellence, dElectrical Engineering Department, Amirkabir University of Technology, 424 Hafez. Ave, Tehran, Iran

Prispelo (Arrived): 17.03.2009 *Sprejeto (Accepted): 09.09.2009*